

On the measurement of Adler angles in charged current single pion neutrino-nucleus interactions

F.Sánchez^{1, a)}

Institut de Física d'Altes Energies (IFAE), The Barcelona Institute of Science and Technology, Campus UAB. 01893 Bellaterra (Barcelona) Spain.

(Dated: 25 September 2018)

Uncertainties in modeling neutrino-nucleus interactions are a major contribution to systematic errors in Long Base Line neutrino oscillation experiments. Accurate modeling of neutrino interactions requires additional experimental observables such as the Adler angles which carry information about the polarization of the Δ resonance and the interference with non-resonant single pion production. The Adler angles were measured with limited statistics in bubble chamber neutrino experiments as well as in electron-proton scattering experiments. We discuss the viability of measuring these angles in neutrino interactions with nuclei.

I. INTRODUCTION

The next generation of Long Base Line (LBL) accelerator neutrino oscillation experiments^{1,2} aims at the discovery of CP violation in the lepton sector and the determination of the neutrino mass hierarchy. Systematic errors are likely to limit the accuracy of these measurements because the energy region of this new generation of experiments, ranging from 0.5 to 10 GeV, is dominated by several poorly measured cross-section channels: charged and neutral current quasi-elastic scattering, single-pion production, multi-pion resonant production and collective nuclear responses such as short and

long range nuclear correlations³. Additional challenges are our incomplete understanding of the nuclear effects contributing to the cross-section and inaccuracies in reconstructing the neutrino energy.

In neutrino oscillation experiments, accurate measurements of oscillation parameters demand that uncertainties arising from the errors on neutrino fluxes and from the neutrino interactions themselves be properly factorized. In turn, this requires the correct modeling of neutrino-nucleus cross sections channels. Neutrino cross-section knowledge suffers from three levels of uncertainties: i) Cross-sections at the nucleon level are not perfectly known. Vector form factors are derived from electron scattering,

^{a)}fsanchez@ifae.es

but axial and pseudoscalar form factors are assumed to be dipolar and constrained by the PCAC hypothesis. ii) Cross-sections are modified by effects due to the nuclear medium through short- and long-range correlations and by uncertainties in nucleon kinematics inside the nucleus. iii) The particles produced in the primary interaction cross the high-density nuclear medium which alters the particle composition of the event. Experimentally, the picture is confused even further by the typically broad neutrino energy spectrum and by beam flux uncertainties. During the last decade efforts were focused on the description and measurement of quasi-elastic scattering; however we now also need to accurately model interactions occurring at higher energies such as single pion production. These data are sparse and contradictory even at the nucleon level⁴. In addition, current and future measurements can be performed only on nuclei.

In this paper, we explore the possibility of measuring Adler angles⁵ in neutrino charged-current pion production on nuclei. A full description of the theoretical implications of Adler angles measurements can be found in the references⁶.

Experimental results from electron scattering on hydrogen have been published by the CLAS^{7,8} collaboration and previously by earlier experiments⁹. These results were ob-

tained on hydrogen targets, thereby avoiding initial and final state nuclear interactions and with the advantage of knowing the initial electron kinematics. Here, we discuss the possibility of measuring these angles in modern neutrino experiments, which are typically performed in broad-band beams and using heavy nuclear targets. In these experiments the neutrino energy must be reconstructed from the data, the initial target nucleon is not at rest and the final state particles undergo nuclear re-scattering.

This work is based on the NEUT¹⁰ Monte Carlo model, described in the following section. The angular observables are illustrated next, followed by Monte Carlo results and conclusions.

II. MONTE CARLO MODEL

Neutrino interactions are simulated with the NEUT¹⁰ program libraries, which include neutral current (NC) and charged current (CC) processes of elastic and quasi-elastic scattering, meson exchange currents, single meson production, single gamma production, coherent pion production and non-resonant inelastic scattering.

NEUT uses the Rein-Sehgal¹¹ model to simulate neutrino-induced single pion production and an *ad-hoc* model for multiple pion production up to a hadronic invariant

mass of $2.0 \text{ GeV}/c^2$. NEUT also includes a contribution from non-resonant pion production and the Δ polarization values measured in deuterium¹².

Final State Interactions (FSI) of hadrons taking place within the nuclear medium are also simulated using a microscopic cascade model. In the case of final state pions, the considered processes are inelastic scattering, pion absorption and charge exchange. The simulated nucleon interactions are elastic scattering as well as single and double Δ production. FSI interactions alter both the multiplicity of pions in the final state as well as the kinematics of the pions.

For the current evaluation, events are generated with a T2K neutrino spectrum¹³. The simulation includes all channels present in the NEUT Monte Carlo. Most current experiments measure neutrino cross-sections on carbon-based detectors, such as plastic scintillator (Polystyrene). To avoid confusion between hydrogen and carbon targets, we decided to study interactions on carbon nuclei. In the case of Polystyrene there will be an additional $\approx 15\%$ of interactions occurring with a free proton, in which the neutrino energy and the Adler angles will be well-determined, except for detector effects.

We consider both the Δ^{++} and the Δ^+ decaying to a π^+ because they are indistinguishable at the experimental level for most

of the final state nucleon momenta.

III. ADLER ANGLES

The Adler reference system⁵ describes the $p\pi^+$ final state in the $p\pi^+$ reference system. The two angles are defined as in Fig.1, where ϕ and θ are sensitive to the transverse and longitudinal polarization of the $p\pi^+$ system for interactions mediated by a Δ^{++} , Δ^+ and for non-resonant contributions. The two angles are properly defined at the nucleon interaction level but they are altered by the Final State Interactions and the Fermi momentum of the target nucleon.

A. Adler angles at the level of the nucleus

Modern experiments detect neutrino interactions on targets consisting of relatively heavy nuclei (carbon, oxygen, iron, argon); therefore the definition of the Adler angles needs to be modified. The first modification is mandated by the fact that normally the proton is not detected. In this case, the $p\pi^+$ reference system needs to be redefined based on detector observables, namely the lepton and the π^+ . In addition, we reconstruct the neutrino energy assuming that the target nucleon is at rest, thereby ignoring its intrinsic Fermi momentum, and assuming that the

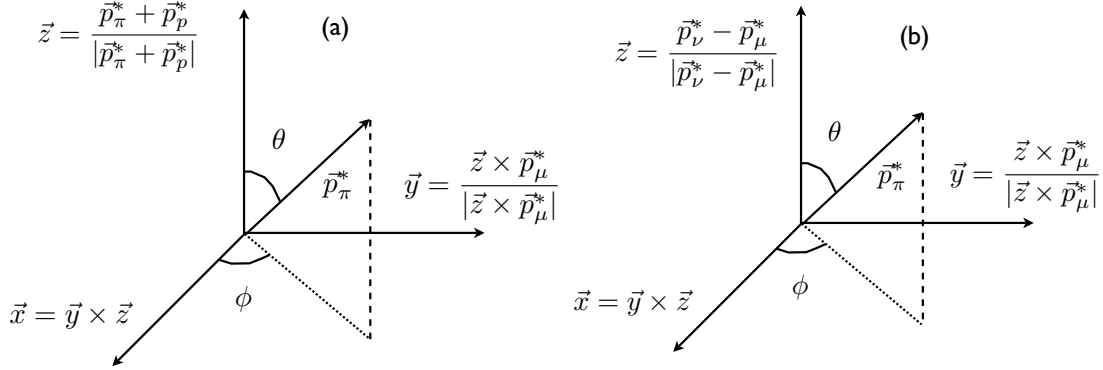


FIG. 1. Definition of the Adler Angles at the nucleon (true) level (a) and the nuclear level (b). The momenta of the particles are defined in the $\vec{q} = \vec{p}_\nu - \vec{p}_\mu$ rest frame.

neutrino direction is known. In this scenario, energy-momentum conservation allows to estimate the neutrino energy as :

$$E_\nu = \frac{m_p^2 - A_p^2 + |\vec{p}_\mu + \vec{p}_\pi|^2}{2(A_p + \vec{d}_\nu \cdot (\vec{p}_\mu + \vec{p}_\pi))}$$

$$A_p = m_p - E_{bind} - E_\mu - E_\pi$$

where (E_μ, \vec{p}_μ) and (E_π, \vec{p}_π) are the four-momenta of the muon and the pion, \vec{d}_ν is the neutrino direction, E_{bind} is the target nucleon binding energy (≈ 25 MeV in NEUT for a carbon target) and m_p is the free proton mass. The target nucleon momentum cannot be inferred when the outgoing proton is not detected. The uncertainty introduced by this approximation will be discussed later. This definition of the neutrino energy and the assumption that the target nucleon is at rest allow us to calculate the invariant

mass of the p- π system and to estimate the values of the observables used in deuterium experiments^{12,14}. We approximate the direction of the final p- π^+ system by the momentum transfer to the nucleus ($\vec{q} = \vec{p}_\nu - \vec{p}_\mu$). The angle between the true p- π^+ system and the estimated \vec{q} is shown in Figure 2. Under the aforementioned assumptions this approximation causes a bias of about 0.2 rad.

The same observables can be reconstructed for the cases of $\Delta^- \rightarrow n\pi^-$ and $\Delta^0 \rightarrow p\pi^-$ to measure the Delta polarization in anti-neutrino nucleus interactions.

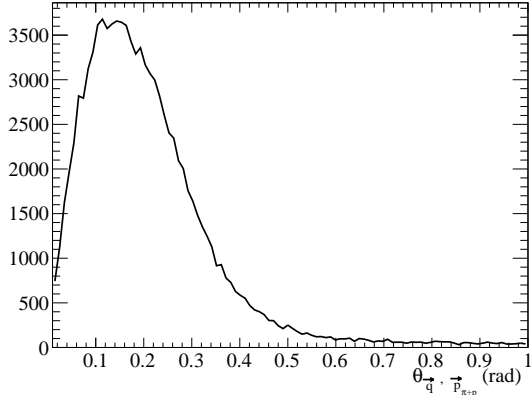


FIG. 2. Angle between the $\vec{p}_p + \vec{p}_\pi$ system and the \vec{q} approximation at the level of the nucleus.

B. Fermi momentum versus Final State Interactions

To evaluate the relative contributions to the Adler angles of the Fermi momentum and the FSI, we compute the Adler angles under three assumptions: **i) true:** we estimate the parameters using the full kinematic information at the level of the nucleon. These results are experimentally measurable only with a hydrogen target. **ii) pre-FSI:** we use the true kinematics of the pion at the level of the nucleon but we ignore the target nucleons momentum. In this case the effect of the Fermi momentum is taken into account but the FSIs are ignored. **iii) post-FSI:** we use the information of the pion leaving the nucleus and ignore the kinematic information of the target nucleon. These are the actual experimental observables and they contain the effect of both the Fermi momentum and of

the FSI.

IV. MONTE CARLO PREDICTIONS

A. Selection of events and their categories

Events are identified from the interactions at the nucleon level and from the multiplicity of particles leaving the nucleus. For the first criterion we rely on the Monte Carlo code to tag single pion production events, produced resonantly or not according to the model of Rein and Sehgal¹¹. In order to assign the multiplicity of the pion final state we look for the number of π^+ , π^- , π^0 and e^\pm emitted by the nucleus, after the FSI. We define a one- π^+ topology when one and only one π^+ is emitted by the nucleus and no other particle from the above list is present. We do not count emitted protons, neutron and nuclear gammas because they are often produced but in current experiments they are detected with low efficiency. Nuclear de-excitation gammas play a negligible role in the description of the neutrino-nucleus interactions discussed here.

The one- π^+ events are then divided into three categories according to the true type of nucleon interaction: i) single pion production, the signal we want to study ii) deep inelastic scattering iii) other processes: for

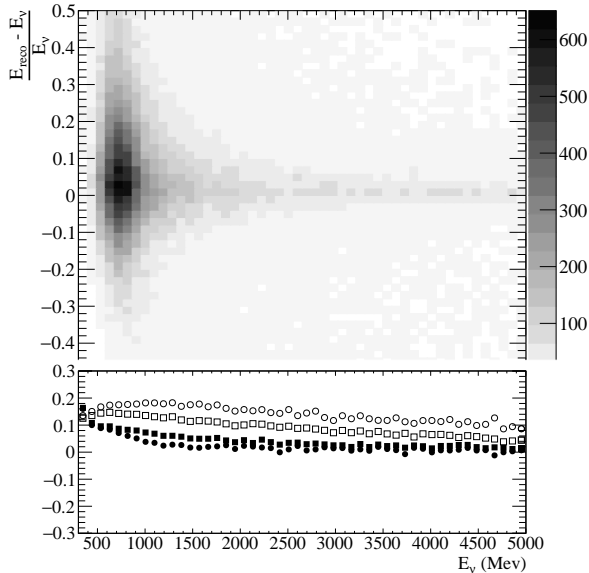


FIG. 3. Relative spread of the reconstructed neutrino energy $(E_{reco} - E_\nu)/E_\nu$ as a function of the true neutrino energy. The black circles (squares) represent the mean value of the relative difference post(pre)-FSI. The empty circles (squares) show the RMS of the reconstructed neutrino energy relative error post(pre)-FSI.

example, η and kaon production. In what follows the last two categories are considered background. The fraction of true charged-current one- π^+ reactions in which a single π^+ emerges from the nucleus is $\sim 75\%$. In $\sim 43\%$ of them the pion momentum is altered by FSI. The background is estimated to be $\sim 18\%$ of single π^+ events leaving the nucleus. These numbers depend on the error on the actual neutrino flux and on the MC models; they only have indicative value.

B. Neutrino energy and hadronic invariant mass reconstruction

The relative spread of the reconstructed neutrino energy is shown in Figure 3 as a function of the neutrino energy. At low energy, due to the relatively large contribution of the target nucleon Fermi momentum, the bias is large, but it decreases from 10% to almost zero at higher neutrino energies due the reduced contribution of the targets Fermi momentum to the total interaction energy. The RMS error is also larger at low energies where it reaches 20% while it decreases to 10% for high neutrino energies. Opposite to other observables, the reconstructed pre-FSI energy is biased towards higher values of energy than the post-FSI reconstruction. The FSI compensates, through the pion energy loss inside the nucleus, the effect of the Fermi momentum decreasing the reconstructed energy.

A cut on the invariant mass of the $p-\pi^+$ system was suggested in the original paper⁵, and applied by the deuterium experiments^{12,14} to constrain the reactions into the region dominated by the $\Delta^{++}(1232)$ resonance. Estimating the neutrino energy allows to obtain the invariant mass of the $p-\pi$ system, taken to be the $\mu - \nu$ invariant mass (W_{reco}), see Figure 4. The plot shows the contribution of the different backgrounds; the deep inelastic background dominates at high

invariant mass values. The invariant mass threshold ($W > 2$ GeV) that defines the DIS region in NEUT is clearly seen in Figure 4. This seems to indicate that the reconstructed W value is a sensitive observable in validating the implementation of the transition from multi-pion production to DIS in the Monte Carlo.

The accuracy of the reconstruction is shown in Figure 5. The invariant mass reconstruction shows a small bias ($< 4\%$) over almost the full range of W and also a relatively small RMS error ($\sim 8\%$). The figure also shows the contribution of the Fermi momentum (black squares) and the combined effect of Fermi momentum and FSI (black circles). The bias (below 1200 MeV) in the reconstructed W is mainly caused by the Fermi momentum of the target nucleon.

C. Reconstructed Adler angles

The reconstructed Adler angles are shown in Figure 6. The true distributions (solid line) are computed for all interactions at the nucleon level and the reconstructed distributions (dotted line) are shown for all events with a single pion leaving the nucleus.

This first look at the result allows to reach some preliminary conclusions: the transverse coordinates (ϕ) are almost unaffected by nuclear effects while the longitudinal observable

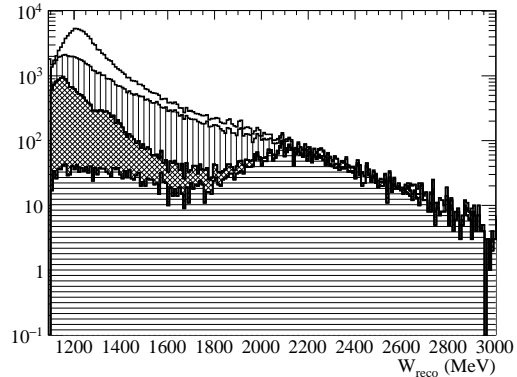


FIG. 4. Reconstructed hadronic invariant mass. The empty histogram shows the CC one- π events. The vertical line histogram shows the invariant mass when the pion momentum is modified by the FSI. The horizontal line histogram shows the CC-DIS contribution to the CC one- π^+ sample and the mesh-filled histogram shows the remaining backgrounds.

(θ) is modified by the change in momentum of the outgoing pion. Background events tend to accumulate at low values of θ while π^+ rescattering events accumulate at high values of θ as it is shown in Figure 6

The difference between the reconstructed and the true ϕ angle is shown in Figure 7. The average bias is close to zero while the maximal RMS error is nearly 1.2 rad. The dependence on the true ϕ angle can be explained by the fact that angles around 0 and π rad correspond to pions contained in the neutrino-muon reaction plane, see Figure 1. These are the cases where the Fermi momen-

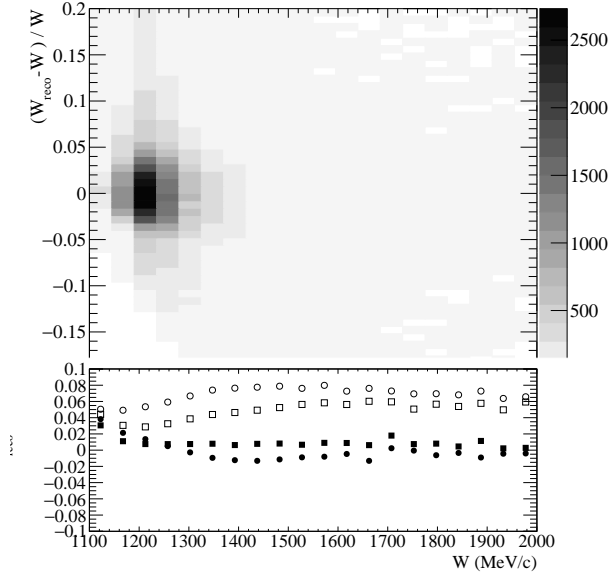


FIG. 5. Relative p - π invariant mass reconstruction error $((W_{reco} - W)/W)$ as a function of the true p - π invariant mass. The black circles (squares) represent the mean value of the relative error post(pre)-FSI. The empty circles (squares) show the RMS of the reconstructed invariant mass relative error post(pre)-FSI.

tion will produce the smallest effect because the true motion of the target nucleon should be contained in the reaction plane. The comparison between the RMS due to the Fermi momentum (0.4 rad) and Fermi momentum plus FSI (1.2 rad), Figure 7, indicates that the main contribution is the re-scattering of pion on its way out of the nucleus.

The dispersion in the reconstructed values of θ is shown in Figure 8. In this case, the bias goes up to 0.15 rad and the RMS is as large as

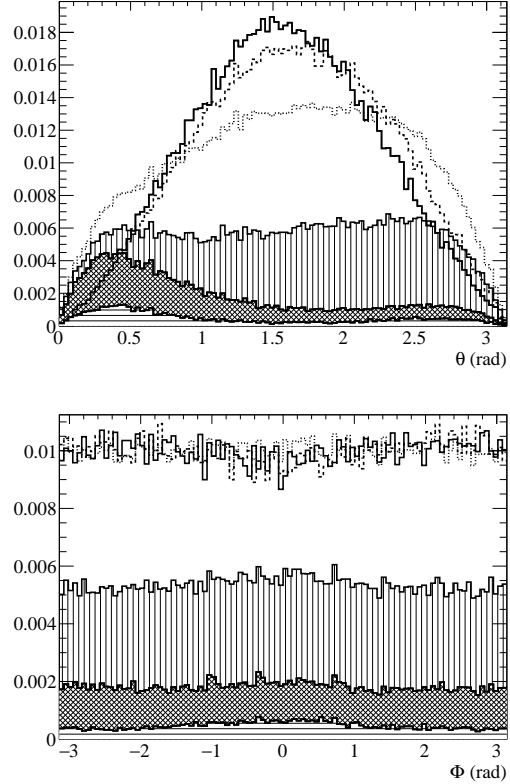


FIG. 6. True (solid line) and reconstructed (dotted line) Adler θ angle (top panel) and ϕ angle (bottom panel). The true CC $1\pi^+$ distributions include all interactions with the target nucleon and the reconstructed ones for those events with pions leaving the nucleus. The dashed line histogram shows the result when the Fermi momentum is ignored in the reconstruction of the true CC $1\pi^+$ result. The histogram filled with vertical lines shows the CC $1\pi^+$ events in which the pion momentum is modified by the FSI. The histogram filled with horizontal lines is the CC-DIS contribution to the CC $1\pi^+$ sample and the histogram filled with a mesh contains the rest of the backgrounds. The distributions are normalized to unity.

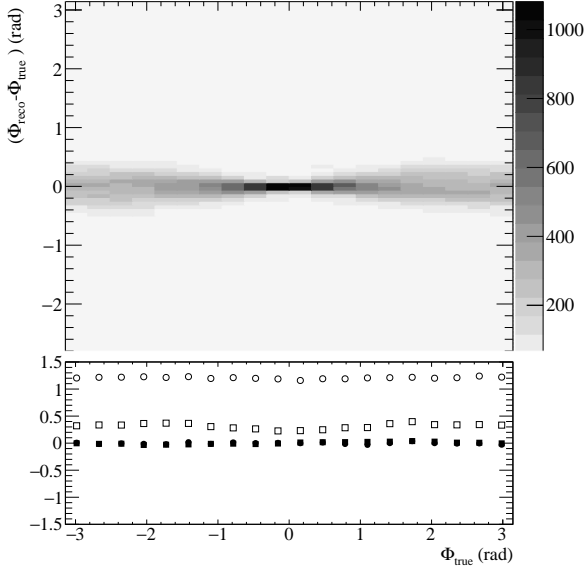


FIG. 7. Reconstructed ϕ angle minus the true ϕ as a function of the ϕ angle. The black circles (squares) show the mean value of the difference post(pre)-FSI. The empty circles(squares) points show the RMS of the difference post(pre)-FSI.

0.4 rad. One can see that θ is very sensitive to the accuracy of the neutrino energy reconstruction and the intranuclear scattering of the charged pion. The FSI are the dominant contribution to the RMS of θ over its whole range.

V. BIAS IN ASYMMETRY MEASUREMENTS

We estimated the potential bias in the reconstruction of the Adler angles by means of a toy Monte Carlo. We take the dependence found from the deuterium results cited

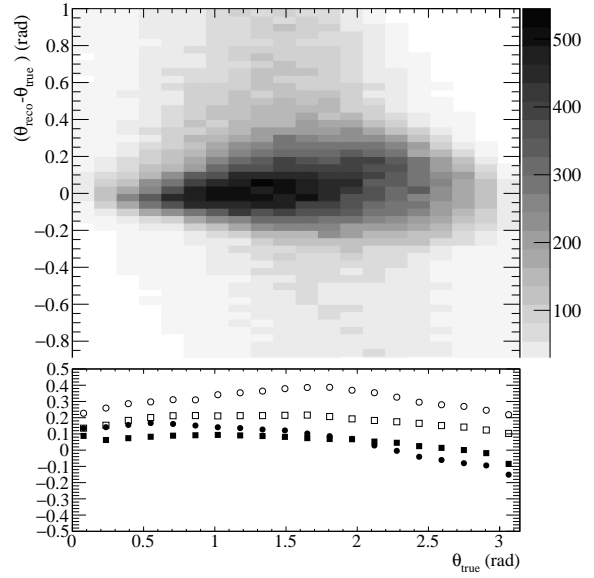


FIG. 8. Reconstructed θ angle minus the true θ angle as a function of θ . The black circles (squares) show the mean value of the difference post(pre)-FSI. The empty circles(squares) show the RMS of the difference post(pre)-FSI.

earlier¹² and weigh the events according to the ϕ angle at the nucleon level with a simple parity-violating function:

$$weight = (1 + \alpha \sin \phi)$$

where α is derived from the asymmetry calculation in the above paper¹² to be 0.083. We fit the same angular dependence for the distributions of the ϕ angle at the nucleon and the nucleus level after subtracting the background and for events with W and W_{reco} below 1400 MeV in order to select events dominated by Δ^{++} and Δ^+ resonant contri-

butions; see Figure 4. The results are shown in Figure 9. The fitted α values, 0.082 ± 0.004 at the nucleon level and 0.053 ± 0.005 at the nucleus level are similar. The errors shown only include the effects of the Monte Carlo statistics. For the reconstructed ϕ , we have subtracted the non-CC $1\pi^+$ interactions. Background modeling will introduce an additional source of uncertainty that is not evaluated in this study.

The bias in the determination of the asymmetry was estimated by generating several ϕ functional dependencies and adjusting the angular dependence. The results are shown in Table I. Although there is a bias in the determination of the α parameter caused by the smearing of the reconstructed ϕ angle, there is still sensitivity to the determination of α . An accurate experimental measurement should consider the variation of the polarization with the event kinematics⁶. Table I shows the result when we take into account the effect of the Fermi momentum. The effect of the Fermi momentum seems to be negligible at this level, as expected from Figure 7. The same calculation was performed for an angular dependence of the type $(1 + \alpha \sin 2\phi)$. The results are shown in Table II. The results are worse than in the previous case due to the convolution with the reconstructed ϕ RMS of the faster oscillation frequency.

We have also estimated the bias in the

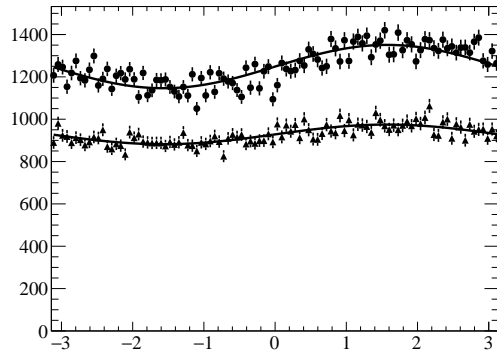


FIG. 9. ϕ distribution at the nucleon (black dots) and nucleus (black triangles) levels weighted by the angular dependence as described in the text. The solid line is the result of the fit to the function $A(1 + \alpha \sin \phi)$

forward-backward asymmetry. Events are not reweighted and the asymmetry is computed as:

$$A_{FB} = \frac{N_{\cos \theta > 0} - N_{\cos \theta < 0}}{N_{\cos \theta > 0} + N_{\cos \theta < 0}}$$

for the distributions of θ both at the nucleon and the nucleus levels, after removing the background. The values of the resulting asymmetries are: -0.007 ± 0.003 (as predicted by the NEUT Monte Carlo) and -0.179 ± 0.003 from the reconstructed observable. The observed bias is produced by the FSI and Fermi momentum within the nucleus because the Adler θ is very significantly modified, as shown in Figure 6. The dependence of the θ angle on the FSI and Fermi momentum makes it a very useful observable

TABLE I. The values of the angular dependence fits (α) for different values of transverse polarization and $\sin\phi$ dependence. Results are shown for pions before and after the FSI.

post-FSI			pre-FSI	
α_{true}	α_{reco}	$\frac{\alpha_{true}-\alpha_{reco}}{\alpha_{true}}$	α_{reco}	$\frac{\alpha_{true}-\alpha_{reco}}{\alpha_{true}}$
0.02	0.0166 ± 0.0050	-0.17	0.0248 ± 0.0055	0.243
0.04	0.0285 ± 0.0050	-0.29	0.0440 ± 0.0055	0.101
0.06	0.0404 ± 0.0050	-0.32	0.0632 ± 0.0055	0.054
0.10	0.0644 ± 0.0050	-0.36	0.1015 ± 0.0054	0.015
0.12	0.0763 ± 0.0050	-0.36	0.1206 ± 0.0054	0.005
0.18	0.1121 ± 0.0050	-0.38	0.1781 ± 0.0053	-0.011

TABLE II. The values of the angular dependence fits (α) for different values of transverse polarization and $\sin 2\phi$ dependence. Results are shown for pions pre- and post-FSI.

post-FSI			pre-FSI	
α_{true}	α_{reco}	$\frac{\alpha_{true}-\alpha_{reco}}{\alpha_{true}}$	α_{reco}	$\frac{\alpha_{true}-\alpha_{reco}}{\alpha_{true}}$
0.02	0.0078 ± 0.0050	-0.60	0.0129 ± 0.0055	-0.35
0.04	0.0192 ± 0.0050	-0.52	0.0308 ± 0.0055	-0.23
0.06	0.0305 ± 0.0050	-0.49	0.0487 ± 0.0055	-0.19
0.10	0.0531 ± 0.0050	-0.47	0.0845 ± 0.0054	-0.16
0.12	0.0644 ± 0.0050	-0.46	0.1024 ± 0.0054	-0.15
0.18	0.0983 ± 0.0050	-0.45	0.1561 ± 0.0054	-0.13

when investigating the nuclear effects on the results of the reaction.

VI. CONCLUSIONS

We have shown that it is possible to measure the Adler angles in neutrino-nucleus scattering. The results based on the NEUT

Monte Carlo show that one can determine the transverse polarization of the Δ resonance because the information is reasonably well maintained despite the FSI and the need to reconstruct the energy of the incoming neutrino from the experimental data. The longitudinal polarization is shown to depend strongly on the kinematics of the emerging

pion, but it appears to allow investigating the effects of pion re-scattering, high mass resonances and deep inelastic processes on the CC one- π^+ tracks emerging from the nucleus. The results indicate that current high-statistics experiments can explore complex observables like Adler angle as a function of the kinematic parameters of the scattering process such as the energy of the neutrino, the hadronic invariant mass and four-momentum transfer.

ACKNOWLEDGMENTS

The author acknowledges the support received from the Ministerio de Economía y Competitividad under grants FPA2014-59855 and Centro de Excelencia Severo Ochoa SEV-2012-0234, some of which include FEDER funds from the European Union. He would like to to acknowledge support from Y. Hayato on the NEUT Monte Carlo, discussions with J. Nieves on the implications of Adler angle measurements and help from S. Bordoni and M. Cavalli-Sforza in revising this paper.

REFERENCES

¹T. Ishida (Hyper-Kamiokande Working Group), “T2HK: J-PARC upgrade plan

for future and beyond T2K,” (2013), arXiv:1311.5287 [hep-ex].

²C. Adams *et al.* (LBNE), “The Long-Baseline Neutrino Experiment: Exploring Fundamental Symmetries of the Universe,” (2013), arXiv:1307.7335 [hep-ex].

³J. Nieves, I. Ruiz Simo, and M. J. Vicente Vacas, “Inclusive Charged-Current Neutrino-Nucleus Reactions,” *Phys. Rev.* **C83**, 045501 (2011), arXiv:1102.2777 [hep-ph].

⁴C. Wilkinson, P. Rodrigues, S. Cartwright, L. Thompson, and K. McFarland, “Re-analysis of bubble chamber measurements of muon-neutrino induced single pion production,” *Phys. Rev.* **D90**, 112017 (2014), arXiv:1411.4482 [hep-ex].

⁵S. L. Adler, “Photoproduction, electroproduction and weak single pion production in the (3,3) resonance region,” *Annals Phys.* **50**, 189–311 (1968).

⁶E. Hernandez, J. Nieves, and M. Valverde, “Weak Pion Production off the Nucleon,” *Phys. Rev.* **D76**, 033005 (2007), arXiv:hep-ph/0701149 [hep-ph].

⁷K. Park *et al.* (CLAS), “Cross sections and beam asymmetries for $\vec{e}p \rightarrow en\pi^+$ in the nucleon resonance region for $1.7 \leq Q^2 \leq 4.5(\text{GeV})^2$,” *Phys. Rev.* **C77**, 015208 (2008), arXiv:0709.1946 [nucl-ex].

⁸H. Egiyan *et al.* (CLAS), “Single π^+ electroproduction on the proton in the first and

- second resonance regions at $0.25 \text{ GeV}^2 < Q^2 < 0.65 \text{ GeV}^2$ using CLAS,” Phys. Rev. **C73**, 025204 (2006), arXiv:nucl-ex/0601007 [nucl-ex].
- ⁹H. Breuker *et al.*, “Forward π^+ Electroproduction in the First Resonance Region at Four Momentum Transfers $q^2 = 0.15(\text{GeV}/c)^2$ and $0.3(\text{GeV}/c)^2$,” Nucl. Phys. **B146**, 285–302 (1978).
- ¹⁰Y. Hayato, “A neutrino interaction simulation program library NEUT,” Acta Phys. Polon. **B40**, 2477–2489 (2009).
- ¹¹D. Rein and L. M. Sehgal, “Neutrino Excitation of Baryon Resonances and Single Pion Production,” Annals Phys. **133**, 79–153 (1981).
- ¹²G. Radecky, V. Barnes, D. Carmony, A. Garfinkel, M. Derrick, *et al.*, “Study of Single Pion Production by Weak Charged Currents in Low-energy Neutrino d Interactions,” Phys. Rev. **D25**, 1161–1173 (1982).
- ¹³K. Abe *et al.* (T2K), “T2K neutrino flux prediction,” Phys.Rev. **D87**, 012001 (2013), arXiv:1211.0469 [hep-ex].
- ¹⁴S. Barish, M. Derrick, T. Dombeck, L. Hyman, K. Jaeger, *et al.*, “Study of Neutrino Interactions in Hydrogen and Deuterium: Inelastic Charged Current Reactions,” Phys. Rev. **D19**, 2521 (1979).